Biomicrofluidics

Biomicrofluidics. 11(5): 054101

Novel functionalities of hybrid paper-polymer centrifugal devices for assay performance enhancement

M. S. Wiederoder[1,2], http://orcid.org/0000-0002-3688-1845S. Smith[1], P. Madzivhandila[1], D. Mager[3], K. Moodley[1], D. L. DeVoe[2], http://orcid.org/0000-0002-8803-8809K. J. Land[1]a)

1. Council for Scientific and Industrial Research, Pretoria, South Africa

2. University of Maryland, College Park, Maryland 20742, USA

3. Karlsruhe Institute of Technology, Karlsruhe, Germany

a) KLand@csir.co.za

DOI: 10.1063/1.5002644
Published online: 12 September 2017

Abstract

The presented work demonstrates novel functionalities of hybrid paper-polymer centrifugal devices for assay performance enhancement that leverage the advantages of both paper-based and centrifugal microfluidic platforms. The fluid flow is manipulated by balancing the capillary force of paper inserts with the centrifugal force generated by disc rotation to enhance the signal of a colorimetric lateral flow immunoassay for pathogenic *E. coli*. Low-cost centrifugation for pre-concentration of bacteria was demonstrated by sample sedimentation at high rotational speeds before supernatant removal by a paper insert via capillary force after deceleration. The live bacteria capture efficiency of the device was similar to a commercial centrifuge. This pre-concentrated sample when combined with gold nanoparticle immunoconjugate probes resulted in a detection limit that is 10× lower than a non-concentrated sample for a lateral flow immunoassay. Signal enhancement was also demonstrated through rotational speed variation to prevent the flow for on-device incubation and to reduce the flow rate, thus increasing the sample residence time for the improved capture of gold nanoparticle-bacteria complexes in an integrated paper microfluidic assay. Finally, multiple sequential steps including sample pre-concentration, filtration, incubation, target capture by an integrated paper microfluidic assay, silver enhancement and quenching, and index matching were completed within a single device. The detection limit was 10^5 colony forming units per ml, a 100× improvement over a similar paper-based lateral flow assay. The techniques utilize the advantages of paper-based microfluidic devices, while facilitating additional functionalities with a centrifugal microfluidic platform for detection performance enhancement in a low-cost, automated platform amenable to point-of-care environments.

I. INTRODUCTION

Paper microfluidic devices demonstrate great potential for commercially viable low-cost point-of-care (POC) diagnostics.[1–3] The developed paper devices are lightweight, disposable, portable, and can include dry reagent storage for simple POC use.[4] The fluid flow is controlled by the capillary force of the substrate facilitating sample flow without external pumps which are common to other microfluidic platforms.[5–7] Other advantages include the ease of fabrication,[8] compatibility with biological samples,[5] well-characterized surface functionalization techniques,[9] and the ability to filter out large aggregates (greater than paper pore size) common in real-world samples that can interfere with the assay.[10] The porous nature of the paper also generates relatively short characteristic diffusion lengths that enhance the capture of target species for certain types of assays to enhance signal for detection.[7]

While paper substrates exhibit numerous advantageous qualities, they have inherent limitations that prevent common laboratory operations such as flow rate control, valving, and metering that are feasible with other microfluidic platforms. The flow rate is dependent on the properties of the substrate, primarily the capillary force, preventing the manipulation of incubation times to enhance the assay signal.[7] Most paper devices utilize a two-dimensional geometry with limited surface area for reagent storage and exhibit unidirectional flow from wet to dry areas that hinders assay complexity.[11] For lateral flow based assays, in particular, all liquids must run through the same passage constraining the number of sequential steps feasible with one device.[5] Numerous studies have tried to overcome these limitations with elements such as 3-dimensional designs with multiple layers,[1,12] integrated timing mechanisms,[11,13–15] or off device sample preparation to reduce total sequential steps on the device. These complex techniques introduce complications in fabrication and often require well-trained users that may prevent adoption for POC applications.

To overcome these problems, some studies have demonstrated the integration of paper microfluidic devices within centrifugal microfluidic platforms. Centrifugal microfluidics or lab-on-a-disc devices rely on an automated rotational motor to manipulate fluid flow through channels by means of centrifugal forces. This enables common microfluidic functionalities that typically require external pumps or manual user steps, so that they are suitable for POC applications without highly trained users.[16] The thermoplastic discs can be made using high-throughput injection or blow molding with inexpensive materials for low-cost, disposable POC applications.[17–19] Devices can contain multiple chambers for sealed reagent storage, employ valves for greater sequential metering of reagents than

paper alone, and allow precise control of fluid flow using automated rotational speed adjustment.[20–22] Unfortunately, thermoplastic substrates limit the performance of some POC assays due to challenging immobilization chemistries and planar surfaces that limit the surface density of specific capture probes for target recognition.[23,24] By integrating paper elements, the total capture probe density increases due to more efficient surface chemistries and the inherent 3-D porous network of paper to enhance performance.[25,26] In addition, balancing the rotational centrifugal force with the capillary force of paper inserts facilitates manipulation of the flow rate and directionality not possible with paper alone. The deceleration and acceleration of the hybrid device also induce active mixing not feasible with paper alone that can enhance the assay performance. Hybrid devices have demonstrated applications such as chromatography,[21] plasma extraction and analysis,[5] timing valves for multiple sequential steps,[27] and sample preparation for colorimetric DNA detection[28,29] not possible with either platform by itself.

In this study, we demonstrate novel functionalities of paper-polymer hybrid centrifugal microfluidic devices for fluid flow manipulation to enhance the assay performance. Specifically, we focus on colorimetric lateral flow immunoassays that use gold nanoparticle immunoconjugate probes (AuNPs) for the detection of E. coli O157:H7, a pathogenic Shiga toxin-producing serotype of E. coli of interest in food and environmental samples. For more background on lateral flow assays, please refer to a comprehensive review by Sajid et al.[10] While commercial AuNP based colorimetric lateral flow assays for bacteria are well established, they often exhibit detection limits too high for certain targets.[3,30] Methods to improve the detection limits of AuNP probe based schemes include pre-concentration with immunomagnetic beads and secondary probe enhancement schemes that add extra manual user steps.[30] In this work, the following automated processing steps are explored to utilize paper-based and centrifugal microfluidic technologies for assay performance enhancement:

- Sample preparation: bacteria pre-concentration and debris filtration. Low cost centrifugation for sample pre-concentration was demonstrated by employing rotational centrifugal force for bacteria sedimentation before rotational speed reduction facilitated the removal of supernatant via capillary force by paper inserts. The sample pre-concentration improves the binding efficiency with AuNPs to enhance the signal for an integrated paper-based lateral flow assay. This technique reduces the number of operations performed by a user by replacing manually operated commercial bench top centrifugation and is amenable to low resource environments. The integrated paper then acts as a filter to prevent large debris or aggregates from interfering with that integrated lateral flow assay.

●. Flow speed and direction control. The flow rate and direction were modified by varying the rotational speed to alter the centrifugal force on the fluid wicked by capillary force into a paper insert. At high rotational speeds, no flow occurs within the paper insert allowing automated incubation of bacteria and AuNPs before introduction into the test strip. In addition, the flow rate reduction caused by rotational speed adjustment was shown to increase the optical signal by increasing the sample residence time for the enhanced capture of AuNP-bacteria complexes on the test line of inserted paper lateral flow assays.

●. Integration of multiple automated sequential steps. Multiple automated sequential steps were completed within a paper-polymer hybrid platform for silver enhancement of captured AuNPs and refractive index matching to improve the assay performance. Silver enhancement creates dark micron scale silver aggregates on captured AuNPs followed by controlled quenching to increase the optical signal and reduce the detection limit. Refractive index matching of the fluid within the porous paper substrate allows imaging of the full thickness by minimizing light scattering to increase the signal to noise ratio (SNR). The experiments demonstrate the value of additional assay steps that are difficult to achieve with a paper-based test alone without adding extra user steps[31] or complex fabrication procedures.[1,12]

The developed techniques maintain the advantages of paper-based assays such as high surface capture probe density, portability, low-cost, and manufacturability while facilitating additional functionalities to improve the detection performance without adding additional user steps. Overall, a 100× improvement in the detection limit was observed with the hybrid device compared to a standard lateral flow based assay for E. coli O157:H7.

II. MATERIALS AND METHODS

A. Disc assembly protocol

The completed paper-polymer hybrid centrifugal microfluidic device is shown in Fig. 1. Three layers were made with 1 mm thick polycarbonate (PC) (Naxel) patterned using a Protomat S63 (LPKF Laser and Electronics) milling machine. The top layer consisted of inlet holes and air vents of 1 mm in diameter formed using a drill bit. All layers were cut out from the PC sheet, and the channels were formed on the middle layer using a 1 mm wide contour router tool bit. The milled PC was then deburred along its edges and cleaned with isopropanol and deionized water. Interstitial pressure sensitive adhesive (PSA) (Flexmount DFM 200 Clear V-95) layers were patterned using an Epilog engraver laser cutter (Helix, 75 W). For the PSA, the top layer consisted of a single layer and the bottom layer consisted of two sheets pressed together using a hand roller. Whatman #1 paper (GE

Healthcare) inserts were also laser cut. The 700–800 μm thick cellulose inserts (Merck) were cut 20 mm × 10.3 mm using a guillotine cutter (Biodot). The bottom layer of the PSA was manually aligned and pressed onto the base PC, followed by manual placement of Whatman #1 inserts, and manual alignment and pressing of the middle PC later. These three layers were then bonded by placing the disc into a plastic bag and passing it through a two-sided rubber roller press (ML25, Drytac) multiple times. Following this, Whatman paper and absorbent cellulose inserts for fluid absorption were placed into the device before manual alignment and placement of the top PSA and the top PC layer. The whole disc was then passed through the roller press multiple times. For all tests, the bottom of the rounded sample chamber was 50 mm from the center of the disc in the radial direction.

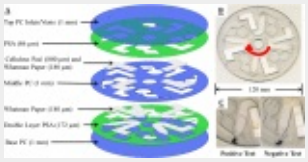

View larger version

FIG. 1. (a) The constructed paper-polymer hybrid device consists of polycarbonate (PC), pressure sensitive adhesive (PSA) and paper inserts. (b) A completed device is shown with the direction of rotation indicated by a red arrow. (c) The paper inset is a colorimetric lateral flow immunoassay with a positive and a negative test result for pathogenic *E. coli* shown in the figure.

The spinning assembly utilized a rotational motor and a controller (Smart Motor SM3450D, Animatics) controlled by Smart Motor Interface software (Animatics) to adjust the rotational acceleration, the rotational speed, and the hold time at a specific speed. The disc was imaged using image capturing software (IC Capture, The Imaging Source) with a CCD camera (DFK 22BUCO3, The Imaging Source) connected to a zoom lens [C1614-M (KP), The Imaging Source]. An optical sensor (D10DPFP), with 0.5 mm fiber optic cable (Banner), was triggered when a reflective foil was passed during rotation to cause a simultaneous strobe flash (DT-311A stroboscope, Shimpo) and image capture.

B. Bacteria concentration study protocol

All reagents were purchased from Sigma Aldrich, unless otherwise specified. E. coli K12 were serially diluted in 40 mM potassium phosphate dibasic (PB) with 1% (w/w) bovine serum albumin (BSA) to study the centrifugation capabilities of the paper-polymer device. Bacteria solution concentration was determined through enumeration on nutrient agar (Oxoid CM0003) after incubation for 24 h at 37 °C. As an experimental positive control, 50 μl of bacteria solution was spun in a 200 μl plastic test tube at 3000 rpm (665 g) for 5 min in a commercial centrifuge (Beckman Coulter, Microfuge16 centrifuge). The rotation speed and duration were chosen based on a previously published protocol with 5 min being the minimum time required for bacterial sedimentation with minimal damage to the living cells.[32–34] Thereafter, 40 μl of supernatant was removed, and the droplet was serially diluted in buffer

before dispensing 100 µl onto nutrient agar for enumeration. For the disc study, 50 µl of bacteria solution was pipetted into the device before spinning at 3000 rpm (504 g) for 5 min at a distance of 50 mm from the center. The device was then spun at 600 rpm (20.16 g) for 10 min to wick the supernatant and leave a concentrated droplet. The concentrated droplet was extracted by piercing the PSA and removing the remaining fluid with a pipette. The volume of this droplet was determined before serial dilution, and the live bacteria count was determined through enumeration on nutrient agar as described previously. The live bacteria capture efficiency was then determined by dividing the number of live bacteria identified in the concentrated droplet by the number of bacteria in the original 50 µl solution.

C. Dipstick test protocol

To test the effect of pre-concentration, a lateral flow dipstick immunoassay was fabricated using Whatman #1 paper. First, Whatman #1 paper was cut and placed on an adhesive backing card (KENOSHA c.v) before patterning 5 µg/ml anti-E. coli O157:H7 antibody per 5 mm to create a 2 mm wide test line. The test strips were incubated for 30 min at 37 °C and then immersed in a commercial blocking solution containing BSA and tween-20 (Invitrogen), padded dry with absorbent towels, and incubated for 1 h at 37 °C. Next, a cellulose absorbent pad was added, and 5 mm wide test strips were cut using a guillotine cutter and shaped to a point at the end using a razor blade to simulate the paper inserts in the disc device.

Gold conjugate solution was prepared by combining 1 ml of 40 nm gold nanoparticles (BBI International) at an optical density of 1 (OD1) with 100 µl of 50 µg/ml anti-E. coli O157:H7 antibodies in 40 mM aqueous PB and incubated for 30 min at room temperature. Next, 1 ml of 0.7% BSA in 40 mM PB (w/w) was added, and the mixture was incubated overnight at 4 °C. The solution was then centrifuged for 15 min at 13 273 rpm (13 000 g), the supernatant was removed, and the mixture was re-suspended in 200 µl of supernatant.

Serial dilutions of E. coli O157:H7 from 104 to 108 colony forming units (CFU)/ml were prepared in aqueous solutions of 1% BSA in 40 mM PB (w/w). The concentration was validated by measuring the solution absorbance at 625 nm (UV/VIS Powerwave HT Spectrophotometer) and comparing it to an established concentration curve calibration (McFarland Standards). To measure the effect of sample concentration, 50 µl of bacteria solution was combined with 3 µl of AuNP conjugate and centrifuged at 3000 rpm for 5 min, after which 40 µl of supernatant was removed. The remaining droplet was vortexed to mix the solution and then incubated for 10 min at room temperature before adding 40 µl of buffer back to the mixture and vortexing. As a positive control, 50 µl of bacteria solution was combined with 3 µl of AuNP conjugate, vortexed, and incubated for 15 min at room temperature.

Thus, the total sample preparation time was 15 min for each test. Next, 50 µl of the selected bacteria test solution was dispensed into a test tube. A test strip was inserted into the test tube with the point facing downward, and the solution was allowed to wick for 10 min. Following this, the test strip was dipped for 10 min in 50 µl of buffer for rinsing to ensure that AuNP-bacteria complexes passed the test line. The test strip was then inserted into an ESEQuant lateral flow test reader (Qiagen) for colorimetric analysis of the test line signal. The relative absorbance of the test line was determined by the following equation:

$$\text{Relative Absorbance } (RA) = I_{\text{test}} - \frac{I_{b1} + I_{b2}}{2}, \tag{1}$$

where I_{test} is the average measured intensity (a.u.) of a region of interest (ROI) 1.5 mm wide over the test line and I_{b1} and I_{b2} are the average background intensity (no capture antibodies) of an equal sized ROI on each side of the test line equidistant from the test line center. For all tests, the limit of detection (LOD) was defined by a confidence interval less than 1% using the Clinical and Laboratory Standards Institute standard, where the limit of blank (LOB) equals the mean blank plus 1.645(SD blank) and the LOD equals LOB plus 1.645(SD low concentration sample).[35]

For comparison and validation, a traditional lateral flow test strip consisting of a cellulose absorbent and an application pad, a glass fiber conjugate pad (Millipore), and a nitrocellulose capture pad (Millipore) was formed.[31] The test strip was inserted into a test tube containing 50 µl of test solution (bacterial dilutions or negative control without bacteria) for 10 min. The resulting test strip was inserted into the ESEQuant lateral flow test reader, imaged, and the relative absorbance was calculated as described above.

D. Spin speed test protocol

A paper insert was printed with a test line as described in Sec. II C to create an integrated lateral flow assay. A solution of E. coli O157:H7 was prepared in aqueous solution of 1% BSA in 40 mM PB (w/w) as described previously in Sec. II B. A volume of 50 µl of test solution was combined with 3 µl of AuNP conjugate and incubated for 15 min before insertion into the test device using a pipette. The device was spun at 0, 200, 400, and 600 rpm for 10 min and then stopped. The length of time required to wick the entire volume was measured using a timer and visualized during spinning to determine when the droplet was fully absorbed. A volume of 50 µl of 1% BSA in 40 mM PB was inserted and the device was spun again at 0, 200, 400, and 600 rpm for 10 min. This was done to ensure that any remaining E. coli-conjugate complexes pass over the test line. The device was then imaged on a

flatbed scanner and analyzed using ImageJ (v1.48, National Institutes of Health, USA) to determine intensity. The relative absorbance was calculated using Eq. (1) with a ROI on the test line and a same sized ROI on either side of the test line equidistant from the test line center.

E. Full assay with silver enhancement protocol

All solutions were manually pipetted into the device inlet before commencing with the spinning steps, with all dilutions of E. coli O157:H7 prepared as discussed above. First, 50 µl of the test solution or a negative control (test solution without bacteria) was combined with 3 µl of the AuNP conjugate in the inlet chamber. The disc was then spun at 3000 rpm for 5 min to concentrate bacteria and AuNPs before spinning at 1500 rpm for 10 min for further incubation to form bacteria-AuNP complexes. Next, the disc was rapidly decelerated to mix the solution and then spun at 600 rpm to wick the sample into the paper insert before stopping for 1 min. Following this, 40 µl of buffer was added, and the disc was spun at 600 rpm for 10 min for rinsing before deceleration to induce mixing and let the remaining fluid absorb into the paper. Next, silver enhancement was performed by combining 20 µl of 2 mg/ml silver acetate in deionized water with 20 µl of 5 mg/ml hydroquinone in citrate buffer[36] in the sample chamber before spinning at 200 rpm for 8 min and stopping for 1 min. Thereafter, the silver enhancement reaction was quenched by adding 30 µl of 3% sodium thiosulfate (w/w) and spinning at 200 rpm for 5 min before stopping for 1 min to complete solution wicking.[37] Finally, refractive index matching of the paper was performed by adding 100 µl of vegetable oil and spinning at 1000 rpm for 15 s to fill the sample chamber before stopping and wicking for 15 min to fully displace the aqueous solution.[38] The disc was imaged on a flatbed scanner after AuNP-bacteria conjugate capture, after silver enhancement and quenching, and after index matching. The RA of the test line and the LOD were determined as described previously.

III. RESULTS AND DISCUSSION

A. Device optimization

The device design required optimization of fabrication methods, geometric design, and experimental parameters to accomplish the study goals. Whatman paper was chosen instead of nitrocellulose commonly employed in lateral flow assays due to the ease of fabrication into custom serpentine shapes, improved wettability for flow control, fiber consistency for index matching, cost (~$2500 per m^2 vs ~$15 per m^2), and ease of integration into the multilayer device for these proof of concept demonstrations. With a paper thickness of 180 µm, a single layer of the PSA (86 µm thickness) was insufficient to create a properly sealed microchannel. Thus, a double layer of two PSA sheets pressed

together was created before laser cutting to minimize air bubbles between the layers. The absorbent cellulose pads were 700–800 μm thick, necessitating an additional layer of Whatman paper to ensure fluid transfer in the 1 mm thick PC layer. The volume of fluid that could be absorbed was dependent on the size of the paper inserts and the absorbent cellulose pads. The described Whatman paper inserts absorbed approximately 60 μl of fluid, and the cellulose absorbed approximately 200 μl before saturation prevented the fluid flow. There was minimal evaporation during testing to affect the flow rate, unlike typical paper microfluidic devices reducing the effect of environmental conditions on the flow rate. Each device contained four distinct reaction chambers to increase the assay throughput. More chambers would be feasible with smaller solution volumes that require less absorption capacity. The shape of the paper insert was tapered to a pointed end to prevent non-uniform fluid absorption during deceleration when the fluid would move circumferentially in the chamber. Previous studies have shown equilibrium between the centrifugal force and the capillary force of Whatman 1 inserts at a rotational speed of 1500 rpm.[21] However, with the tapered end at the force equilibrium, no fluid flow occurred at 1000 rpm due to the reduction in the paper surface area in contact with the sample. All of these factors influenced the final designs presented in Secs. III B–III E.

B. Bacteria concentration

To validate bacteria pre-concentration from a liquid sample, the constructed hybrid paper-polymer devices were compared to a standard commercial centrifuge. E. coli K12 suspended in buffer was chosen as a model system to simulate biological samples common in waste water sanitation verification procedures.[39] For the experiments, 50 μl of solution was spun at 3000 rpm for 5 min for sample sedimentation before deceleration and spinning at 600 rpm for 10 min for supernatant removal by the paper insert. The droplet volume extracted from the hybrid device was 8–10 μl, and the droplet volume after manual supernatant removal from the commercial centrifuge tube was 10 μl. The live bacteria capture efficiency was 67%–71% (6.7–7.1× increase in concentration) for the commercial centrifuge and 46%–51% (4.6–5.1× increase in concentration) for the hybrid device (Fig. 2). The commercial centrifuge captures more live bacteria than the hybrid device with significant concentration increase for both methods. Higher rotation speeds were attempted (Table S1, supplementary material), but the live bacteria efficiency decreased due to increased loss of viability for enumeration on agar with higher rotational forces. Reasons for the decreased bacterial capture efficiency with the hybrid device include loss due to absorption into the paper during initial acceleration, a small difference in g-force, and incomplete fluid extraction. For the purposes of immunoassays, both viable and non-viable bacteria have affinity for the antibody probes used to generate binding complexes. Thus, it is likely that there are even more bacteria in the concentrated

droplet that could be detected than just those enumerated on nutrient agar. Others have demonstrated bacteria pre-concentration using centrifugal microfluidics for fluorescent assay enhancement using a siphon valve for supernatant removal.[40] However, in contrast to the presented work, the study employed off device filtration and sample pre-concentration with a commercial centrifuge before introduction into the device. Furthermore, the use of siphon valves in combination with integrated paper based assays would require complex fabrication and reduce available real-estate on a centrifugal platform. The paper insert also acts as a filter to remove large aggregates for sample preparation commonly needed for real-world samples in environmental, food, and medical applications that would remain when only using a siphon valve. The technique suggests that a paper-polymer hybrid device could act as a low-cost centrifuge for sample preparation in POC environments without an existing commercial device either as a stand-alone step or in combination with a subsequent assay.

View larger version

FIG. 2. Average live bacteria capture efficiency of *E. coli* K12 using a commercial centrifuge or hybrid paper-polymer device at 3000 rpm (n = 3 with error ±1 SD). The direction of disc rotation is indicated by a red arrow.

C. Pre-concentration of sample on a dipstick

The effect of sample concentration was evaluated using a Whatman #1 paper-based lateral flow immunoassay dipstick. Dilutions of E. coli O157:H7 were combined with AuNPs and either pre-concentrated in a commercial centrifuge or incubated without centrifugation. The 40 nm diameter AuNPs settle along with the bacteria in the test tube, concentrating both in a volume that is 20% of the original solution. For pre-concentrated samples, the LOD was 10^6 CFU/ml, a 10× reduction over the non-centrifuged sample (Fig. 3). For comparison, the LOD of the traditional lateral flow assay described in the Methods section with the same reagents, and no bacteria pre-concentration was 10^7 CFU/ml. In addition, the relative absorbance of the test line was greater for the centrifuged sample compared to a non-centrifuged sample at each concentration tested. By decreasing the liquid volume that contained the bacteria and AuNPs, the effective diffusion length decreased resulting in the formation of more AuNP-bacteria complexes. Thus, more species were captured on the test line of the lateral flow dipstick improving the performance of the assay. The total time for sample preparation was 15 min for both cases before addition to the lateral flow test strip.

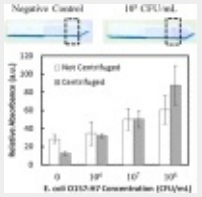

View larger version

FIG. 3. Example Whatman paper lateral flow immunoassays for *E. coli* O157:H7 are shown for a negative control and a 10^8 CFU/ml solution with the test line outlined in black. The average relative absorbance ($RA_{dilution} - RA_{negative\ control}$) is shown with and without sample pre-concentration. N = 3 with error bars ± 1 standard deviation (SD).

D. Rotation speed variation

To examine the effect of rotational speed, a 10^7 CFU/ml solution of E. coli O157:H7 was incubated with AuNPs for 10 min in a test tube at ambient temperature. The solution was pipetted into the inlet of the hybrid paper-polymer device and spun between 0 and 600 rpm for 10 min before rinsing with buffer at the same speed for 10 min. The results show that as the rotational speed and the centrifugal force increases, the time required to fully wick a 50 µl sample increases. While the capillary force remains constant, the increase in the centrifugal force decreases the fluid flow rate through the paper insert. Because the interactions between antibodies on the paper insert and the AuNP-bacteria complexes in solution are diffusion limited, an increase in sample residence time on the test line caused by a decrease in flow rate enhances the optical signal (Fig. 4). At speeds greater than 600 rpm, the total sample wicking time was greater than 10 min with no visible wicking occurring at speeds greater than 1000 rpm. By employing a hybrid platform, the flow rate within the paper microfluidic device can be modified to enhance the signal. Furthermore, while not demonstrated here, it is feasible to use such a platform to create bidirectional flow through speed changes, where AuNP-bacteria complexes pass across the test line multiple times to increase the number of captured species and the optical signal.

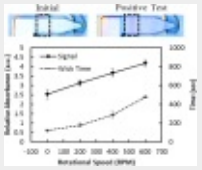

View larger version

FIG. 4. Effect of rotation speed on the wicking time and the relative absorbance of an integrated lateral flow test assay with a sample of 10^7 CFU/ml with test line outlined. Initial conditions and a positive test are shown. For each rotation speed, n = 3 with error bars ± 1 SD.

E. Full study with AuNPs, silver enhancement, and index matching fluid

To demonstrate the developed techniques and additional functionalities of a centrifugal platform, a colorimetric lateral flow immunoassay for E. coli O157:H7 with sequential silver enhancement and index matching steps to improve the performance was implemented (Fig. 5).

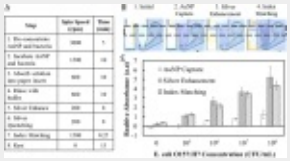

View larger version

FIG. 5. (a) The experimental procedure is described with (b) examples of inserted paper lateral flow assays with the test line outlined in black after the completion of selective procedural steps using a 10^8 CFU/ml solution. (c) The average relative absorbance is shown for each dilution with $N \geq 3$ and error bars ±1 SD.

When using AuNPs alone, the detection limit was 10^6 CFU/ml with a noise floor defined as the negative control (no bacteria) plus three standard deviations. This represents a 10× detection limit improvement on a dipstick test and a standard lateral flow assay with nitrocellulose without pre-concentration and the same detection limit as the pre-concentrated dipstick test with an increase in the signal to noise ratio (Fig. 3). The addition of the silver enhancement step combined with quenching decreased the detection limit 10× to 10^5 CFU/ml. In addition, each dilution tested was statistically significant for each other (Student's t-test $p \leq 0.05$), unlike with AuNPs alone, giving a dynamic range of 3 logs. This demonstrates the potential for quantification of target concentration assays not possible with conventional colorimetric lateral flow assays.[3] The addition of index matching had no effect on the detection limit or dynamic range with a decrease in total intensity of the paper when infused with oil. However, when calculating the signal to noise ratio (SNR) by dividing the average relative absorbance (RA) by the standard deviation at each concentration, the index matching step was found to increase the SNR at each concentration. The total assay took 1 h, with 15 min for the index matching step, and contained up to four test regions on each device.

Silver enhancement reactions occur when silver ions nucleate on AuNPs in the presence of a reducing agent (hydroquinone) and form micron scale silver aggregates. In comparison to recent work with silver enhancement of a lateral flow assay, all steps were automated in this study without manual rinsing or user handling of the device.[31] Because silver enhancement is highly sensitive to incubation time, microfluidic devices often employ multiple manual water rinsing steps or require image capturing within a set time interval. In this study, we introduce a quenching agent that reduces the need for multiple rinsing steps and ensures uniformity across devices and during storage, which is beneficial for many POC applications. The 10× improvement in the LOD is consistent with other studies that use AuNPs and silver enhancement for colorimetric detection.[31,41]

The increase in the SNR by using a refractive index matching fluid is consistent with previous work, where enhanced performance of porous detection elements was demonstrated using an index matching fluid.[26,38,41] By imaging the volume and not just the surface, the SNR increases to improve the assay sensitivity or distinguishable signal change per change in concentration, which in turn improves the

quantification accuracy of an assay. An increase in the SNR should also decrease the LOD, but this was not observed for the tested dilutions of between 10^4 CFU/ml and 10^5 CFU/ml, and thus no such claim is made in this paper. While images were acquired with a white light illuminated flatbed scanner operated in the reflectance mode, the use of an index matching fluid also enables a transmission based set-up with a light source and an optical detector on opposite sides of the device. Transmission based imaging using inexpensive LEDs at optimized wavelengths and inexpensive optical detectors has been demonstrated for more sensitive analyte quantification for paper based tests.[38,42]

The demonstrated experiments are amenable for POC diagnostic platforms with further development using known technologies. On-chip reagent storage either in pre-loaded wells, blister packets, or on the paper insert itself would need to be developed with passive or physical valves for sequential metering, as demonstrated in numerous studies.[43–47] Further optimization of spinning speeds and wait times to increase the incubation length would enhance the signal and decrease the LOD, while increasing the assay completion time. Multiplex testing is also feasible either by printing multiple test lines on a single paper insert or by introducing numerous paper inserts for different targets. Finally, employing enhanced surface chemistry or alternative self-wetting porous substrates for improved capture probe density could be explored to enhance the performance in combination with the previously described techniques.

IV. CONCLUSIONS

This study demonstrates novel functionalities of hybrid paper-polymer centrifugal microfluidic devices to enhance the performance of paper microfluidic assays. The demonstrated immunoassay maintains the advantages of paper microfluidic inserts as a detection element, while adding additional microfluidic functionalities for sample pre-concentration, flow control, active mixing, and integration of numerous sequential assay steps. Low-cost centrifugation compatible with remote environments is demonstrated by rotation at high speeds with centrifugal force for sample concentration followed by speed reduction for supernatant removal by the paper insert using capillary force. The sample pre-concentration increased the binding efficiency of AuNPs with bacteria targets to increase the signal of a colorimetric lateral flow immunoassay. Signal enhancement was also achieved by moderating flow control through centrifugal force generation to increase the sample residence time on the printed test line. Finally, a complete lateral flow assay including sample pre-concentration, incubation, AuNP capture, silver enhancement and quenching, and refractive index matching was demonstrated to achieve a 100× improvement in the detection limit over a dipstick assay alone. All assay steps were

completed in 45 min–1 h using an automated platform minimizing the possibility of user error. Overall, the demonstrated techniques provide further tools to improve the sensor performance for paper-based platforms while maintaining low-cost and inherent user-friendly characteristics.

Supplementary Material

Open In Web Browser

ACKNOWLEDGMENTS

This work was supported by the NSF GRFP under Grant No. DGE1322106, the USAID Research and Innovation Fellows Program, the DFG under Grant No. MA5859/1-1, and the Council for Scientific and Industrial Research (CSIR) in Pretoria, South Africa.

References

1. D. D. Liana, B. Raguse, J. Justin Gooding, and E. Chow, Sensors 12, 11505–11526 (2012).10.3390/s120911505 23112667
2. X. Li, D. R. Ballerini, and W. Shen, Biomicrofluidics 6, 11301–1130113 (2012).10.1063/1.368739 22662067
3. A. K. Yetisen, M. S. Akram, and C. R. Lowe, Lab Chip 13, 2210–2251 (2013).10.1039/c3lc50169h 23652632
4. L. Ge, S. Wang, X. Song, S. Ge, and J. Yu, Lab Chip 12, 3150–3158 (2012).10.1039/c2lc40325k 22763468
5. N. Godino, E. Vereshchagina, R. Gorkin, and J. Ducrée, Microfluid. Nanofluid. 16, 895–905 (2014).10.1007/s10404-013-1283-9
6. P. Shah, X. Zhu, and C. Li, Expert Rev. Mol. Diagn. 13, 83–91 (2013).10.1586/erm.12.13 23256705
7. A. L. Ahmad, S. C. Low, S. R. A. Shukor, W. J. N. Fernando, and A. Ismail, J. Membr. Sci. 357, 178–184 (2010).10.1016/j.memsci.2010.04.018

8. A. Martinez, S. Phillips, G. Whitesides, and E. Carrilho, Anal. Chem. 82, 3–10 (2010).10.1021/ac901398920000334
9. P. Kwong and M. Gupta, Anal. Chem. 84, 10129–10135 (2012).10.1021/ac302861v23113699
10. M. Sajid, A. N. Kawde, and M. Daud, J. Saudi Chem. Soc. 19, 689–705 (2015).10.1016/j.jscs.2014.09.001
11. B. J. Toley, J. A. Wang, M. Gupta, J. R. Buser, L. K. Lafleur, B. R. Lutz, E. Fu, and P. Yager, Lab Chip 15, 1432–1444 (2015).10.1039/C4LC01155D25606810
12. H. Liu and R. M. Crooks, J. Am. Chem. Soc. 133, 17564–17566 (2011).10.1021/ja207177922004329
13. J. H. Shin, J. Park, S. H. Kim, and J. Park, Biomicrofluidics 8, 54121 (2014).10.1063/1.4899773
14. H. Fu, Q. Wu, C. Zhao, X. Li, N. Li-jessen, and X. Liu, in International Conference on Miniaturized Systems for Chemistry and Life Sciences (MicroTAS) (2016), pp. 192–193.
15. S. Huang, S. Bennett, K. Abe, P. Ladd, T. Liang, K. Shah, P. C. Kauffman, S. Paul, M. Purfield, C. E. Anderson, L. Yokobe, B. Strelitz, K. Follmer, K. Pullar, J. Englund, and P. Yager, in International Conference on Miniaturized Systems for Chemistry and Life Sciences (MicroTAS) (2016), pp. 190–191.
16. S. Smith, D. Mager, A. Perebikovsky, E. Shamloo, D. Kinahan, R. Mishra, S. M. Torres Delgado, H. Kido, S. Saha, J. Ducrée, M. Madou, K. Land, and J. G. Korvink, Micromachines 7, 22 (2016).10.3390/mi7020022
17. H. Sharma, D. Nguyen, A. Chen, V. Lew, and M. Khine, Ann. Biomed. Eng. 39, 1313–1327 (2011).10.1007/s10439-010-0213-121152984
18. M. Geissler, E. Roy, G. A. Diaz-Quijada, J.-C. Galas, and T. Veres, ACS Appl. Mater. Interfaces 1, 1387–1395 (2009).10.1021/am900285g20355940
19. D. Desai, G. Wu, and M. H. Zaman, Lab Chip 11, 194–211 (2011).10.1039/C0LC00340A21125097
20. N. Godino, R. Gorkin, K. Bourke, and J. Ducrée, Lab Chip 12, 3281–3284 (2012).10.1039/c2lc40223h22842728
21. H. Hwang, S.-H. Kim, T.-H. Kim, J.-K. Park, and Y.-K. Cho, Lab Chip 11, 3404–3406 (2011).10.1039/c1lc20445a21863153
22. E. Vereshchagina, K. Bourke, L. Meehan, C. Dixit, D. Mc Glade, and J. Ducrée, in MEMS (2013), pp. 1049–1052.
23. C. D. Chin, T. Laksanasopin, Y. K. Cheung, D. Steinmiller, V. Linder, H. Parsa, J. Wang, H. Moore, R. Rouse, G. Umviligihozo, E. Karita, L. Mwambarangwe, S. L. Braunstein, J. van de Wijgert, R. Sahabo, J. E. Justman, W. El-Sadr, and S. K. Sia, Nat. Med. 17, 1015–1019 (2011).10.1038/nm.240821804541
24. J. Wen, X. Shi, Y. He, J. Zhou, and Y. Li, Anal. Bioanal. Chem. 404, 1935–1944 (2012).10.1007/s00216-012-6297-822868478
25. J. Liu, C.-F. Chen, C.-W. Chang, and D. L. DeVoe, Biosens. Bioelectron. 26, 182–188 (2010).10.1016/j.bios.2010.06.00720598520
26. M. S. Wiederoder, L. Peterken, A. X. Lu, O. D. Rahmanian, S. R. Raghavan, and D. L. DeVoe, Analyst 140, 5724–5731 (2015).10.1039/C5AN00988J26160546
27. D. J. Kinahan, S. M. Kearney, O. P. Faneuil, M. T. Glynn, N. Dimov, and J. Ducrée, RSC Adv. 5, 1818–1826 (2015).10.1039/C4RA14887H
28. M. Geissler, L. Clime, X. D. Hoa, K. J. Morton, H. Hébert, L. Poncelet, M. Mounier, M. Deschênes, M. E. Gauthier, G. Huszczynski, N. Corneau, B. W. Blais, and T. Veres, Anal. Chem. 87, 10565–10572 (2015).10.1021/acs.analchem.5b0308526416260
29. T. Kim, J. Park, C. Kim, and Y. Cho, Anal. Chem. 86, 3841–3848 (2014).10.1021/ac403971h24635032
30. S. Shan and W. Lai, J. Agric. Food Chem. 63, 745–753 (2015).10.1021/jf504641525539027
31. M. O. Rodríguez, L. B. Covián, A. C. García, and M. C. Blanco-López, Talanta 148, 272–278 (2016).10.1016/j.talanta.2015.10.06826653449
32. J. A. Harrison and M. A. Harrison, J. Food Prot. 59, 1336–1338 (1996).10.4315/0362-028X-59.12.1336

33. C. Sichel, J. Blanco, S. Malato, and P. Fernandez-Ibanez, J. Photochem. Photobiol., A: Chem. 189, 239–246 (2007).10.1016/j.jphotochem.2007.02.004
34. K. M. Smith and M. A. Lauffer, Advances in Virus Research (Elsevier, 1953), Vol. 1.
35. D. A. Armbruster and T. Pry, Clin. Biochem. Rev. 29(Supp. 1), S49 (2008).18852857
36. G. W. Hacker, L. Grimelius, G. Danscher, G. Bernatzky, W. Mussl, H. Adam, and J. Thurner, J. Histotechnol. 11, 213–221 (1988).10.1179/his.1988.11.4.213
37. C. C. Liu, C. Y. Yeung, P. H. Chen, M. K. Yeh, and S. Y. Hou, Food Chem. 141, 2526–2532 (2013).10.1016/j.foodchem.2013.05.08923870991
38. A. K. Ellerbee, S. T. Phillips, A. C. Siegel, A. W. Mirica, K. A. Martinez, P. Striehl, N. Jain, M. Prentiss, and G. M. Whitesides, Anal. Chem. 81, 8447–8452 (2009).10.1021/ac901307q19722495
39. J. P. S. Cabral, Int. J. Environ. Res. Public Health 7, 3657–3703 (2010).10.3390/ijerph710365721139855
40. J. Litvinov, S. T. Moen, C. Koh, and A. K. Singh, Biomicrofluidics 10, 014103 (2016).10.1063/1.493909926858815
41. M. S. Wiederoder, L. Peterken, O. D. Rahmanian, E. L. Kendall, and D. L. DeVoe, in P5 Africa Congress - Leveraging Point of Care Testing and Personalized Medicine, 2016.
42. C. Swanson, S. Lee, A. J. Aranyosi, B. Tien, C. Chan, M. Wong, J. Lowe, S. Jain, and R. Ghaffari, Sens. Bio-Sens. Res. 5, 55–61 (2015).10.1016/j.sbsr.2015.07.005
43. J. Kim, H. Kido, R. H. Rangel, and M. J. Madou, Sens. Actuators, B 128, 613–621 (2008).10.1016/j.snb.2007.07.079
44. K. Abi-Samra, R. Hanson, M. Madou, and R. A. Gorkin, Lab Chip 11, 723–726 (2011).10.1039/C0LC00160K21103528
45. W. Al-Faqheri, F. Ibrahim, T. H. G. Thio, J. Moebius, K. Joseph, H. Arof, and M. Madou, PLoS One 8, e58523 (2013).10.1371/journal.pone.005852323505528
46. T. Van Oordt, Y. Barb, J. Smetana, R. Zengerle, and F. von Stetten, Lab Chip 13, 2888–2892 (2013).10.1039/c3lc50404b23674222
47. D. J. Kinahan, S. M. Kearney, N. A. Kilcawley, P. L. Early, M. T. Glynn, and J. Ducrée, PLoS One 11(5), e0155545 (2016).10.1371/journal.pone.015554527167376

[Back]

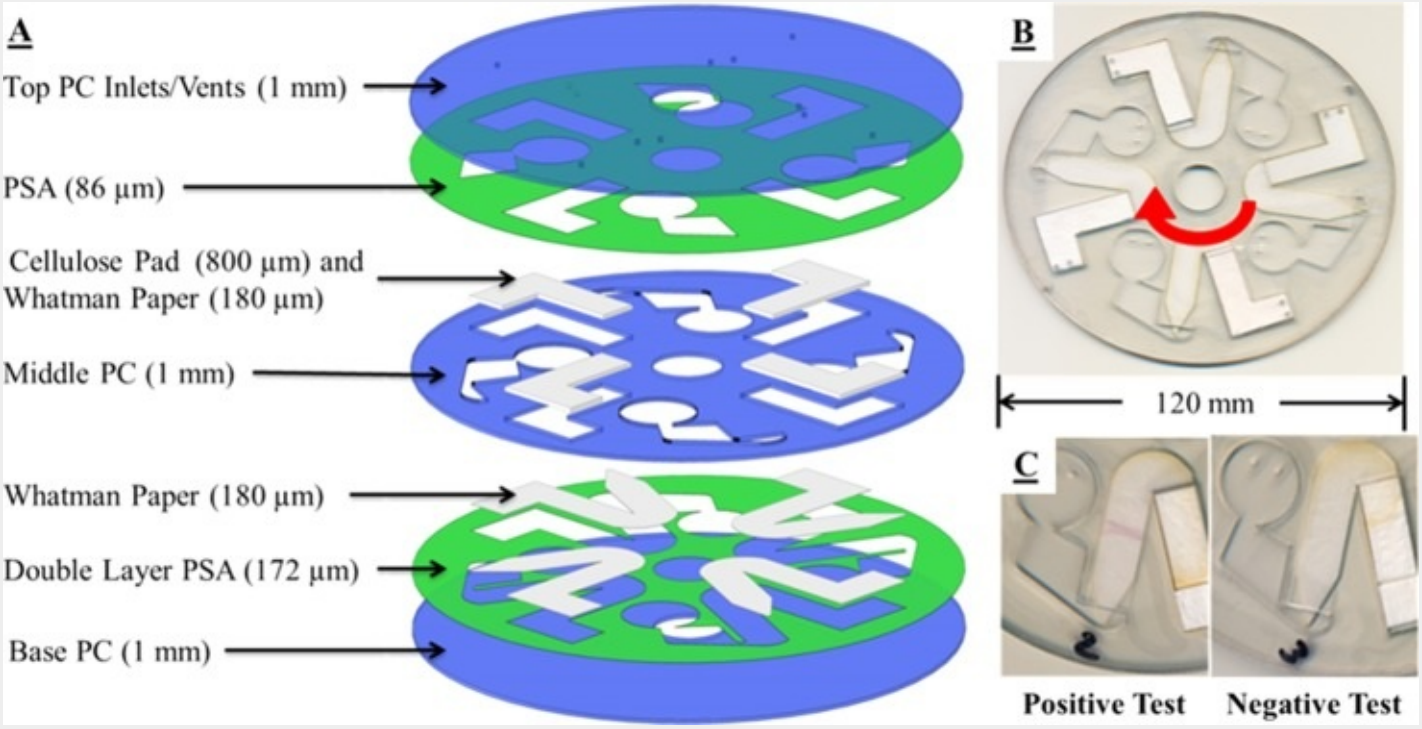

FIG. 1.

(a) The constructed paper-polymer hybrid device consists of polycarbonate (PC), pressure sensitive adhesive (PSA) and paper inserts. (b) A completed device is shown with the direction of rotation indicated by a red arrow. (c) The paper inset is a colorimetric lateral flow immunoassay with a positive and a negative test result for pathogenic *E. coli* shown in the figure.

[Back]

[Back]

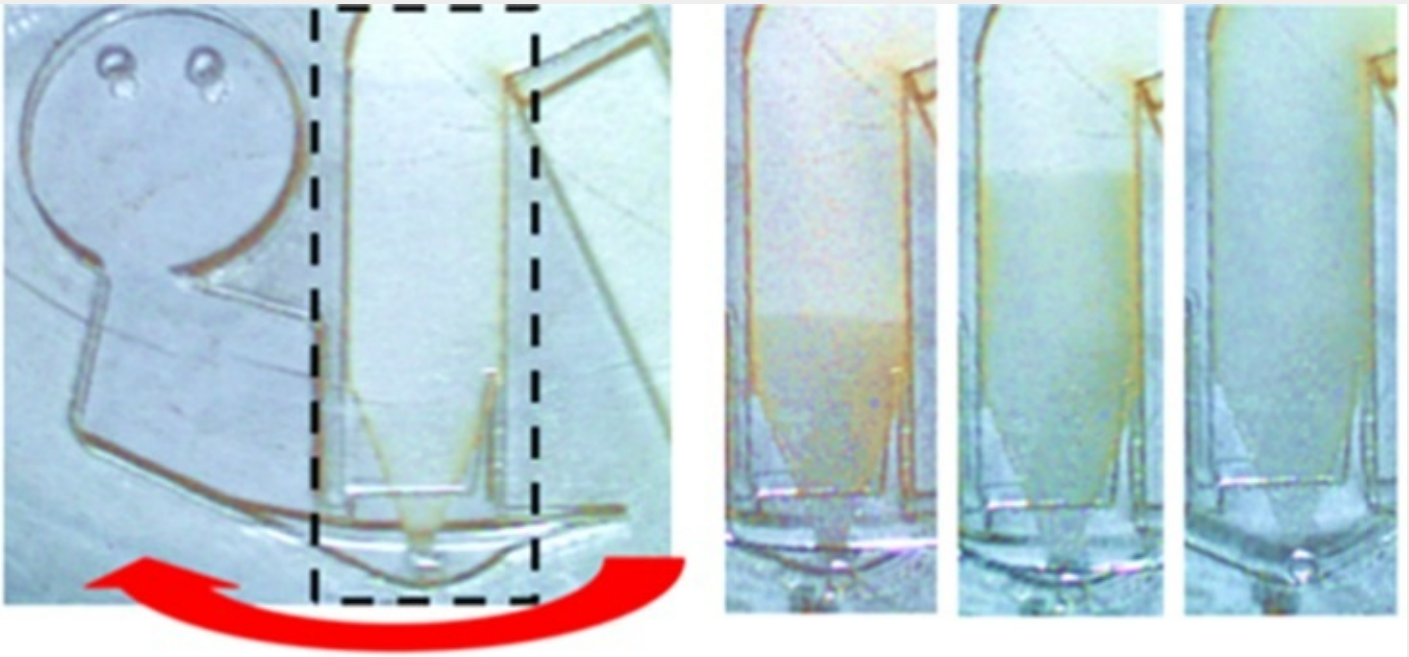

1. Pelletize bacteria (3000 rpm)

2. Remove supernatant (600 rpm)

Live Bacteria Capture Efficiency (%)

Bacteria Concentration (CFU/mL)	3000 rpm	
	Centrifuge	*Hybrid Device*
10^8	71.0 ± 5.5	50.9 ± 9.6
10^7	66.7 ± 9.4	46.2 ± 8.9

FIG. 2.

Average live bacteria capture efficiency of *E. coli* K12 using a commercial centrifuge or hybrid paper-polymer device at 3000 rpm (n = 3 with error ±1 SD). The direction of disc rotation is indicated by a red arrow.

[Back]

[Back]

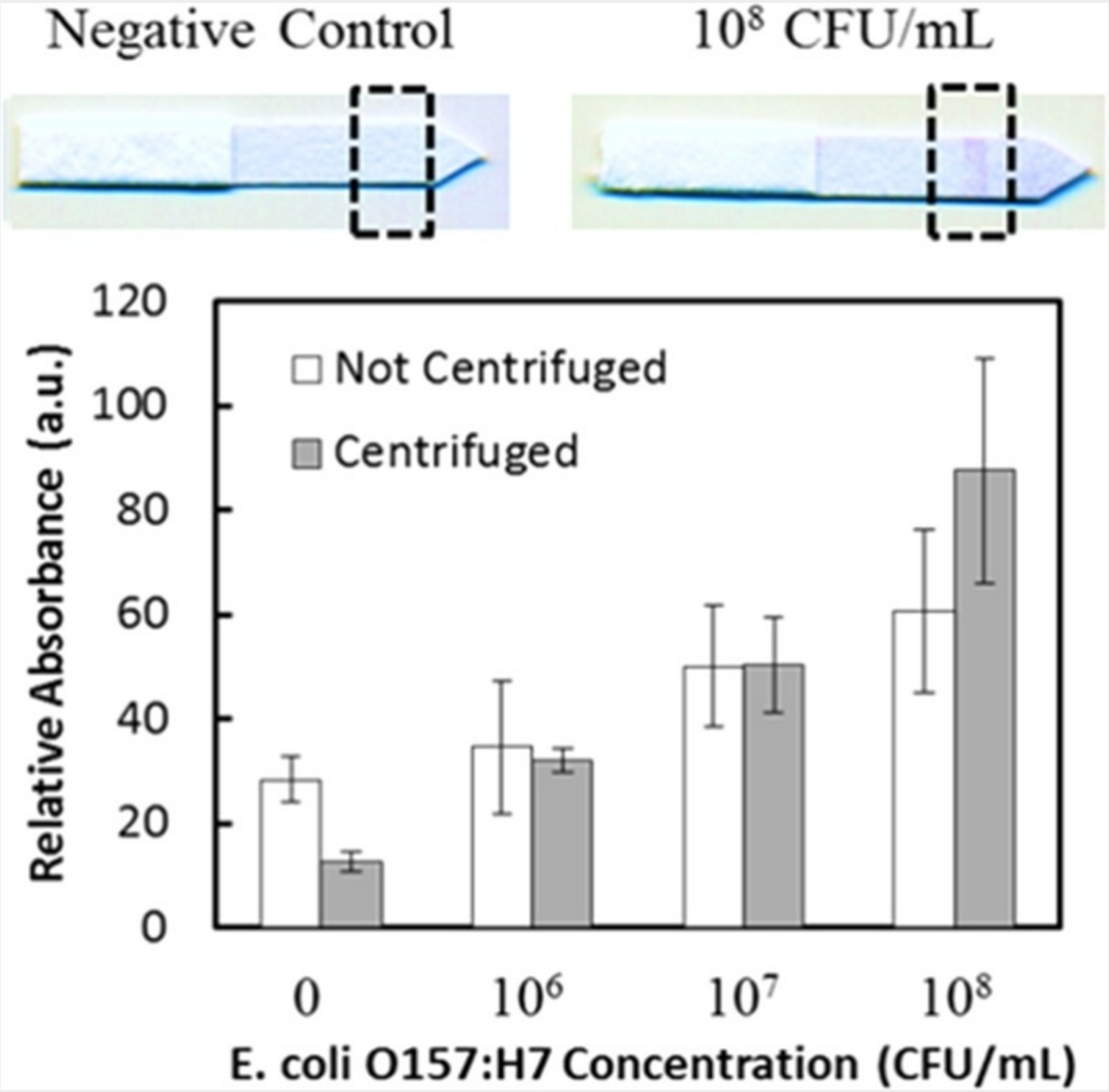

FIG. 3.

Example Whatman paper lateral flow immunoassays for *E. coli* O157:H7 are shown for a negative control and a 10^8 CFU/ml solution with the test line outlined in black. The average relative absorbance ($RA_{dilution} - RA_{negative\ control}$) is shown with and without sample pre-concentration. N = 3 with error bars ± 1 standard deviation (SD).

[Back]

[Back]

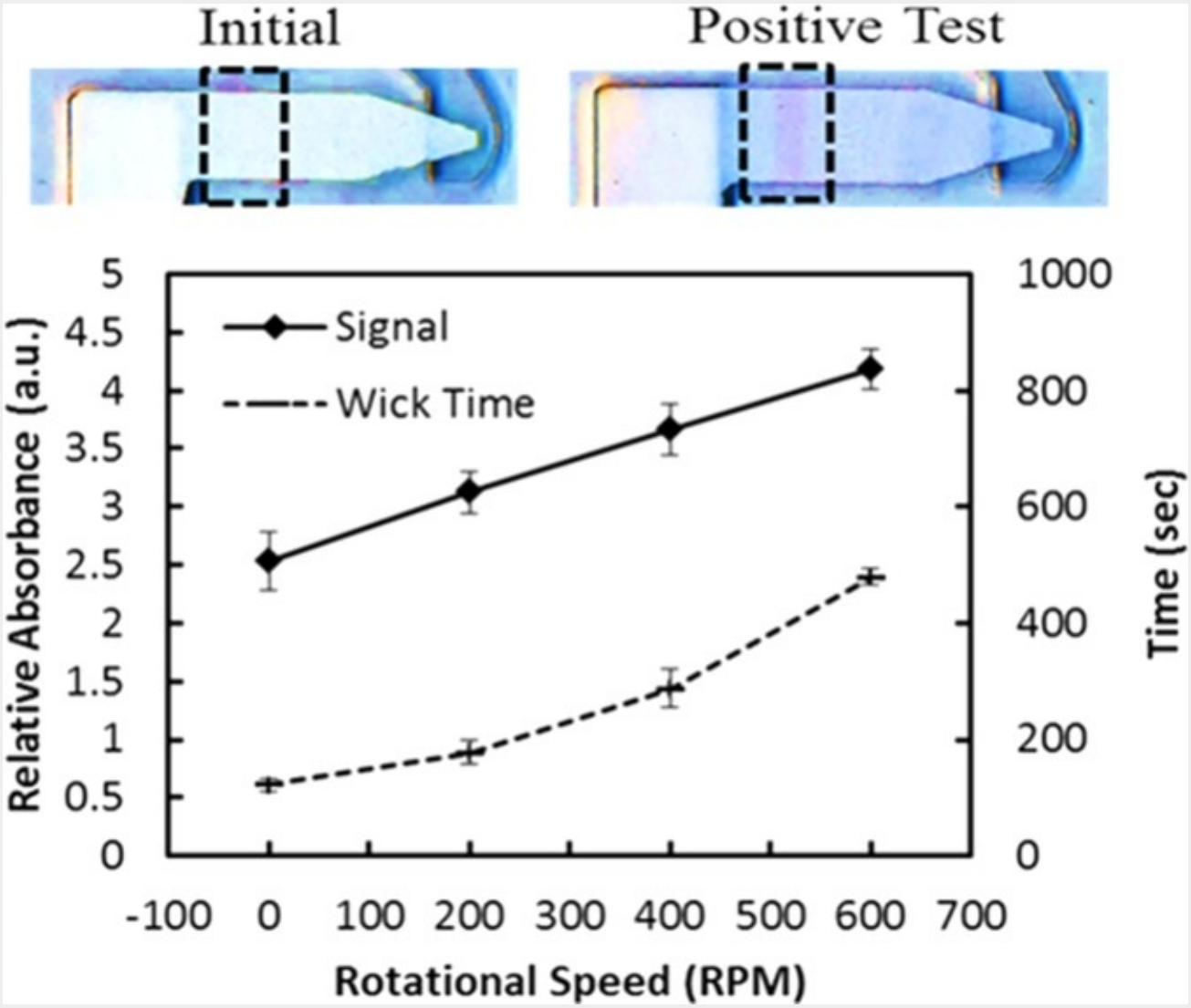

FIG. 4.

Effect of rotation speed on the wicking time and the relative absorbance of an integrated lateral flow test assay with a sample of 10^7 CFU/ml with test line outlined. Initial conditions and a positive test are shown. For each rotation speed, n = 3 with error bars ± 1 SD.

[Back]

[Back]

A

Step	Spin Speed (rpm)	Time (min)
1. Pre-concentrate AuNP and bacteria	3000	5
2. Incubate AuNP and bacteria	1500	10
3. Absorb solution into paper insert	600	10
4. Rinse with buffer	600	10
5. Silver Enhance	200	8
6. Silver Quenching	200	8
7. Index Matching	1500	0.25
8. Rest	0	15

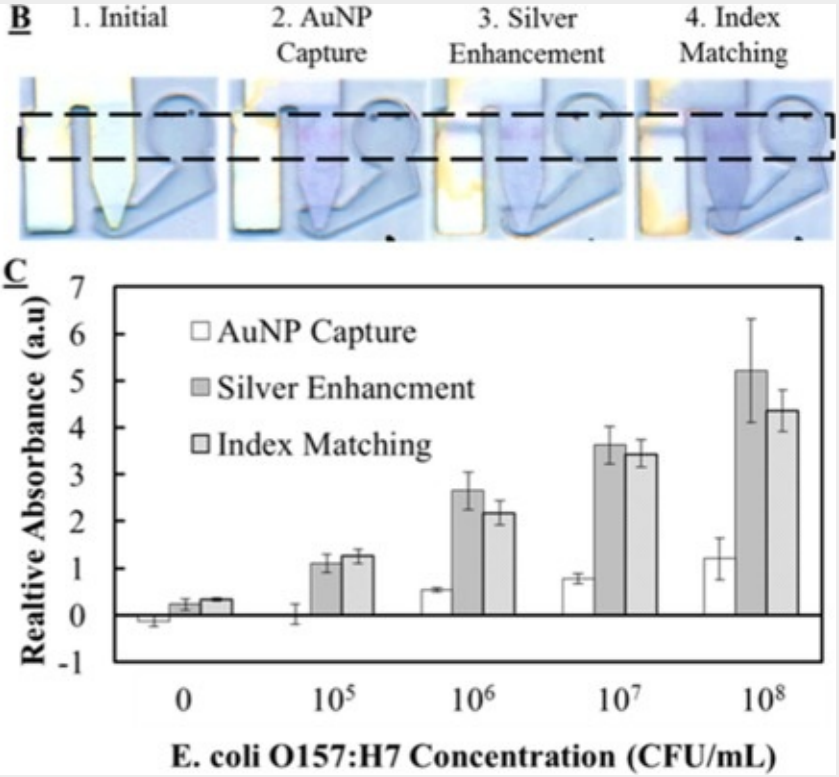

FIG. 5.

(a) The experimental procedure is described with (b) examples of inserted paper lateral flow assays with the test line outlined in black after the completion of selective procedural steps using a 10^8 CFU/ml solution. (c) The average relative absorbance is shown for each dilution with $N \geq 3$ and error bars ±1 SD.

[Back]